Indian Journal of Pure & Applied Physics
Vol. 61, September 2023, pp. 731-734
DOI: 10.56042/ijpap.v61i9.3152

Unravelling the Ultralow Thermal Conductivity of Ternary Antimonide Zintl Phase $RbGaSb_2$: A First-principles Study

Sangeeta, Rajesh Kumar, Ramesh Kumar, Kulwinder Kumar & Mukhtiyar Singh*
Department of Applied Physics, Delhi Technological University, Delhi 110 042, India

Received 28 June 2023; accepted 14 August 2023

The recent discovery of antimonide based Zintl phase compounds has sparked the research in finding high-performance thermoelectric materials. In present study, a ternary antimonide Zintl phase $RbGaSb_2$ is investigated using First-principles calculations. A good agreement observed between our computed results, such as lattice parameter and thermal conductivity, with the experimental report validating our theoretical framework. A direct band gap of 1.17 eV is obtained using Tran Blaha modified Becke Johnson approach. The negative value of Seebeck coefficient indicates its n-type character. We purpose a strategy for enhancing power factor via carrier concentration optimization. The calculated results reveal the anisotropic transport properties. The intrinsic ultralow lattice thermal conductivity about 0.094 $Wm^{-1}K^{-1}$ along the x-direction, and 0.019 $Wm^{-1}K^{-1}$ along z-direction at room temperature is obtained. The ZT value can reach 0.90 (in x-direction) and 0.85 (in z-direction) for n-type doping at 900 K, indicating $RbGaSb_2$ as promising thermoelectric material.

Keywords: $RbGaSb_2$; Ternary Antimonide Zintl Phase; Thermal Conductivity; DFT

1 Introduction

Thermoelectric (TE) materials incorporate an approach that transform thermal energy into electricity without any moving parts and have been identified as highly promising candidates for energy harvesting[1,2]. The efficiency of these materials relies on the figure of merit, ZT, which is represented as $S^2\sigma T/ k_e + k_l$. Here, S, σ, k_e, and k_l denote the Seebeck coefficient, electrical conductivity, electronic thermal conductivity, and lattice thermal conductivity, respectively. Currently, extensive research has been taking pace on various materials[3-5] to explore their potential application in thermoelectricity. Among these, Zintl compounds possess intriguing properties like mix chemical bonding, narrow band gap, and high density of material. Their complex structure leads to low lattice thermal conductivity due to large phonon scattering. Also, these compounds exhibit Phonon-Glass Electron-Crystal behaviour[6,7]. Motivated by the recent experimental synthesis of ternary antimonide $RbGaSb_2$[8], we examine the structural, electronic and transport properties. This work presents an effective n-type Zintl compound with remarkable promise as a future TE material across a large temperature range.

*Corresponding authors: (E-mail: msphysik09@gmail.com)

2 Computational Methods

The properties of $RbGaSb_2$, were analysed using density functional theory based wien2k code[9]. The optimisation of the structure was performed using generalised gradient approximation method proposed by Perdew-Burke-Ernzerhof[10]. An energy convergence of 0.0001 Ry was achieved when the Kohn-Sham equations were solved in a self-consistent manner. For Brillouin zone sampling, a Monkhorst-Pack k-mesh of 17×17×9 was used. The Tran Blaha modified Becke Johnson (TB-mBJ) approach was chosen to perform calculations pertaining to the electronic and transport properties[11]. The transport properties were obtained via solving Boltzmann Transport equation (BTE) as implemented in BoltzTraP code[12]. The phono3py code was used for the computation of anharmonic third-order inter atomic force constants[13]. The lattice thermal conductivity was obtained by solving phonon BTE employing a dense 13 × 13 × 7 q-mesh.

3 Results and Discussion

3.1 Structural and electronic properties

$RbGaSb_2$ ternary antimonide Zintl phase crystallizes in tetragonal structure with space group $P4_2/nmc$ (space group no. 137). The crystal structure as shown in Fig. 1(a) inset, of the investigated compound comprises of two-dimensional $[GaSb_2]^-$

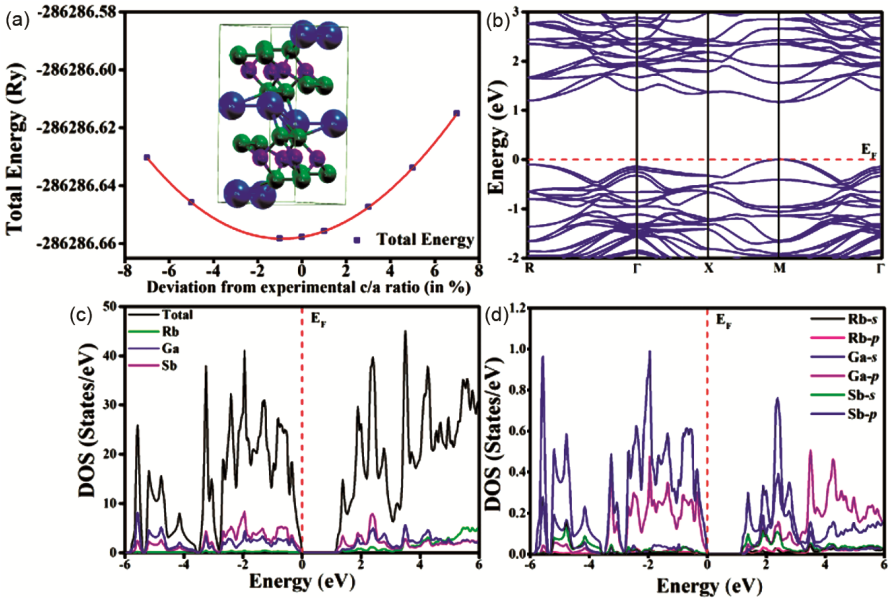

Fig. 1 — (a) The optimization of total energy versus deviation from experimental c/a ratio, Crystal structure (inset). Calculated (b) electronic band structure (c) and (d) density of states of $RbGaSb_2$ using TB-mBJ potential.

tetrahedral layers separated by layer of Rb^+ cations. There are two $[GaSb_2]^-$ layers in the unit cell that are shifted along the [010] direction. This structure results in high degree of anisotropy. The calculated total energy versus deviation from experimental c/a ratio is shown in Fig. 1(a). The initial value of c/a ratio is taken from experimental data (1.857) and optimized value is 1.841. The optimized crystal structure parameters and comparison with the experimental ones are presented in Table 1. The optimised structure is further used to evaluate the electronic and transport properties.

The electronic band structure of $RbGaSb_2$ obtained using TB-mBJ is shown in Fig. 1 (b). The conduction band minima (CBM) and the valence band maxima (VBM), both present at M, indicating a direct band gap. The calculated energy band gap of 1.17 eV is close to previously estimated value of 1.0 eV. It is experimentally found that $RbGaSb_2$ tend to form n-type semiconductor near room temperature[8], therefore we only focus on the lower part of CB that can determine the transport properties of n-type $RbGaSb_2$. The band structure exhibits less dispersion at M k-point in the lower part of CB, suggesting that the electron effective mass is large and high S can be obtained. The density of states is obtained as shown in Fig. 1(c-d). Both VB and CB are predominantly contributed by Sb atoms, while negligible contribution of Rb atoms is observed. The sharp peaks observed at VBM and CBM. Also, the upper part of VB and lower part of CB are majorly contributed by the *p* orbital of Sb atoms.

Table 1– Calculated lattice parameters, volume, and total energy.

	a=b (Å)	c (Å)	Volume (Å^3)	Total energy (Ry)
This work	8.359	15.390	1075.56	-286007.0047
Exp.[8]	8.335	15.483	1075.60	-

3.2 Transport and properties

The transport parameters of $RbGaSb_2$ are computed through the solution of the BTE. We employed rigid band approximation which assumes that temperature and doping concentration have no impact on electronic band structure, and constant relaxation time approximation, which states that S is independent of scattering rate. We have investigated how temperature and electron concentration affect TE coefficients. The variation of the S, σ, k_e and ZT is obtained as functions of electron concentration for both n-type $RbGaSb_2$ in the range 10^{18}-10^{21} cm^{-3} along the [100] (x-direction) and [001] (z-direction) crystallographic directions for temperature 300, 600 and 900 K. The S value decreases with carrier concentration in both directions as shown in Fig. 2(a-b). The negative value of S signifies n-type behaviour of $RbGaSb_2$.

The maximum S value obtained is -633.66 μVK^{-1} in x-direction at 900 K for electron concentration of 1×10^{18} cm^{-3}. Further utilizing the values of electrical conductivity and S we calculated power factor (PF) in terms of relaxation time (τ) at 300, 600, and 900 K in both directions. The PF/τ first increase with the

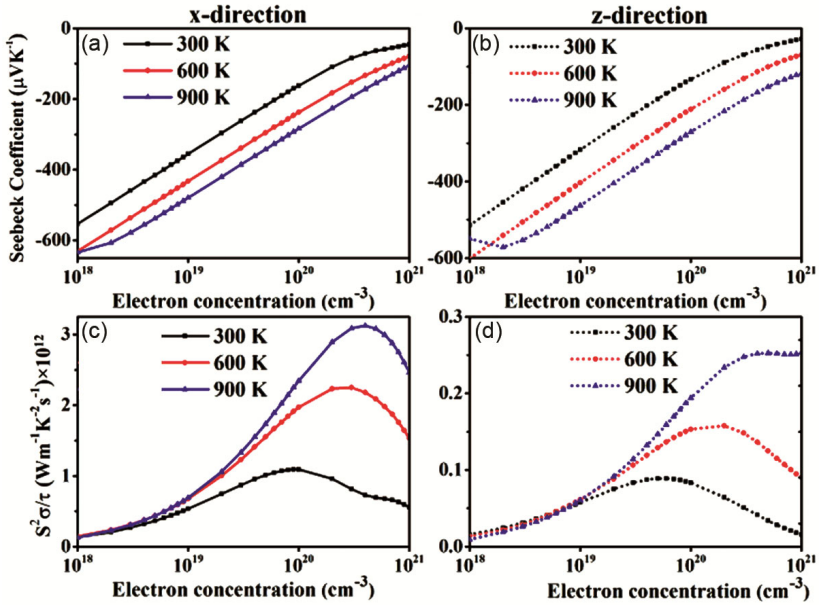

Fig. 2 — Calculated (a-b) Seebeck coefficient, and (c-d) power factor in x- (solid lines) and z- (dotted lines) direction as a function of electron concentration at different temperatures.

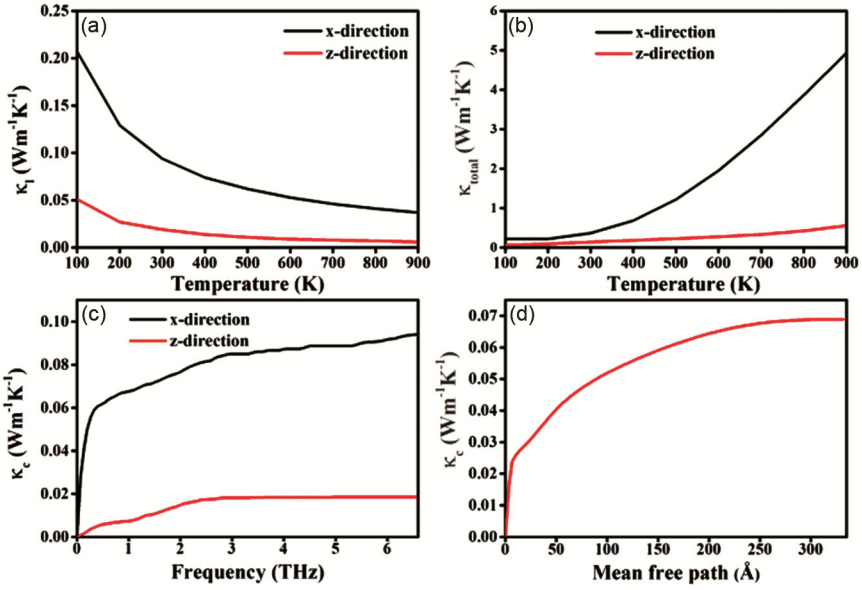

Fig. 3 — Calculated (a) k_l (b) k_{total} (c-d) k_c as a function of frequency and mean free path.

increase in electron concentration then reaches a maximum value, as shown in Fig. 2(c-d). High PF is obtained in x- than z-direction. The optimized PF/τ values at 4×10^{20} cm^{-3} are 3.13×10^{11} (x-direction) and 0.25×10^{11} (z-direction) at 900 K.

Further, to evaluate ZT we calculate k_l that decreases with the increase in temperature in both directions as shown in Fig. 3(a). This decrease in k_l at higher temperatures is attributed to the phenomenon of Umklapp phonon-phonon scattering. The total thermal conductivity, k_{total} (Fig. 3(b)) of $RbGaSb_2$ was found to be 0.38 W/m-K at a temperature of 300 K and found within the range of previously reported values for antimony based TE[14].The complex crystal structure, and rattling behavior of Rb cation and the presence of heavy elements leads to ultralow thermal conductivity of $RbGaSb_2$[15].

The calculated frequency dependent cumulative lattice thermal conductivity (k_c) shown in Fig. 3(b) reveals that low frequency phonon modes contribute

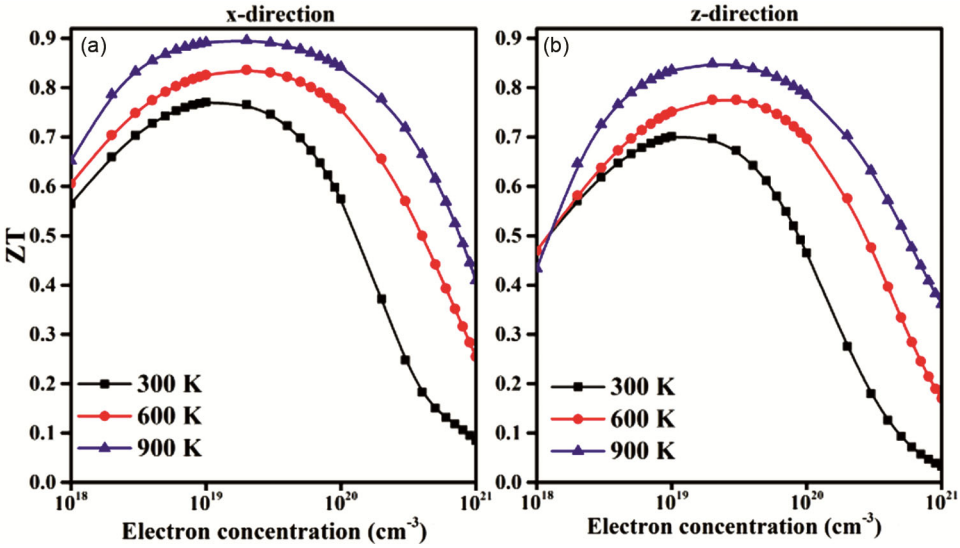

Fig. 4 — Calculated ZT as a function of electron concentration of $RbGaSb_2$ (a) in x-direction (b) in z-direction.

most to k_l in the x-direction and then increases slightly. Fig. 3(b) shows the k_c depends on the mean free path. The variation of ZT with electron concentration at different temperatures is shown in Fig. 4. At a constant temperature, ZT for both directions increase with electron concentration and it reaches optimum value at ~10^{19}cm^{-3}, after that significantly decreases. The maximum ZT values at optimized electron concentration are found to be 0.90 (in x-direction) and 0.85 (in z-direction) at 900 K. The high ZT value of $RbGaSb_2$ is obtained by ultralow k_l and large value of power factor.

4 Conclusion

In summary, we have investigated the electronic structure and TE properties of n-type $RbGaSb_2$ using first-principles calculations and BTE. The key advantage of $RbGaSb_2$ as TE material which is attributed to the complex crystal structure, the potential rattling of Rb cations, and presence of heavy elements. This low thermal conductivity allows for efficient conversion of heat into electricity, making it potential candidate for TE applications.

Acknowledgement

We acknowledge NSM for providing computing resources of 'PARAM SMRITI' at NABI, Mohali, which is implemented by C-DAC and supported by the Ministry of Electronics and Information Technology (MeitY) and Department of Science and Technology (DST), Government of India.

References

1 Xiao Y & Zhao L-D, *Science*, 367 (2020) 1196.
2 He J & Tritt T M, *Science*, 357 (2017) eaak9997.
3 Kumar R, Kumar R, Singh M, Meena D & Vij A, *J Phys D: Appl Phys*, 55 (2022) 495302.
4 Yadav A, Kumar S, Muruganathan M & Kumar R, *EPL*, 132 (2020) 67003.
5 Sangeeta, Kumar R & Singh M, *J Mater Sci*, 57 (2022) 10691.
6 Kauzlarich S M, Brown S R & Jeffrey Snyder G, *Dalton Trans*, (2007) 2099.
7 Chen C, Feng Z, Yao H, Cao F, Lei B-H, Wang Y, Chen Y, Singh D J & Zhang Q, *Nat Commun*, 12 (2021) 5718.
8 Wang J, Owens-Baird B & Kovnir K, *Inorg Chem,* 61 (2022) 533.
9 Schwarz K, Blaha P & Madsen G K H, *Comput Phys Commun*, 147 (2002) 71.
10 Perdew J P, Burke K & Ernzerhof M, *Phys Rev Lett*, 77 (1996) 3865.
11 Tran F & Blaha P, *Phys Rev Lett*, 102 (2009) 226401.
12 Madsen G K H & Singh D J, *Comput Phys Commun*, 175 (2006) 67.
13 Togo A, Chaput L & Tanaka I, *Phys Rev B*, 91 (2015) 094306.
14 Kuo J J, Kang S D, Imasato K, K Tamaki K, Ohno S, Kanno T & Snyder G J, *Energy Environ Sci*, 11 (2018) 429.
15 Toberer E S, Zevalkink A & Snyder G J, *J Mater Chem*, 21 (2011) 15843.